High Performance AC Electroluminescence from Colloidal Quantum Dot Hybrids

*Sung Hwan Cho, Jinwoo Sung, Ihn Hwang, Richard Hahnkee Kim, Yeon Sik Choi, Seoung Soon Jo, Tae Woo Lee, and Cheolmin Park**

Electroluminescent (EL) devices based on solution-processed printable materials that include fluorescent polymers and, more recently, colloidal semi-conducting quantum dots (QDs) are quite attractive for a variety of emerging mobile applications due to their low production costs and potential for fabrication into flexible, large area, lightweight devices.[1–7] In addition to conventional EL device architecture in which EL from either the polymer or QDs is, in principle, achieved by holes and electrons injected from their own ohmic electrodes followed by formation of excitons in the emissive layer that recombine radiatively,[8–11] new EL devices with different mechanisms for emission have been proposed based on alternating current (AC) electric fields.[12–17]

Similarly to well established inorganic electroluminescent devices,[16,17] solution-processible devices are also mechanistically understood as being either solid-state cathode luminescence (SSCL),[18,19] in which EL is achieved by impact excitation of the emitting layer by bombardment of hot electrons accelerated through an inorganic oxide layer, or field-induced luminescence[20,21] where bipolar charges injected from electrodes in an AC field form excitons followed by recombination in the emissive layer. Although recent progress has been made to enhance brightness and to reduce the driving power of AC EL devices including our work in which we employed individually networked single wall carbon nanotubes (SWNTs) dispersed in a fluorescent polymer layer,[13–17] the challenge of fine control of emitting color by mixing still remains as well as that of tuning with further improvement of brightness. This is, we believe, one of the most important issues for further development of solution-processible AC driven EL devices.

Here, we report an efficient route for both color mixing and tuning of AC EL based on solution-processed colloidal QDs and their hybrids with fluorescent polymers. A novel AC EL device was demonstrated containing a thin organic/inorganic hybrid nanocomposite film of colloidal CdSe-ZnS core-shell type QDs blended in a light emitting polymer matrix. Cooperative emission of the two light emitting materials due to unique phase segregated microstructure resulted in extremely bright AC EL of approximately 620 cd/m^2 at an applied voltage and AC frequency of ±55 V and 300 kHz, respectively. Furthermore, the hybrid AC EL device (hereafter denoted as HACEL) which featured an emissive layer composed of a blue poly(9,9-di-n-octylfluorenyl-2,7-diyl) (PFO) polymer and orange QDs exhibited effective color mixing, giving rise to high performance white HACEL. Our simple device platform by solution process also enabled fabrication of a reliable AC EL device capable of color tuning by control of the blend composition.

The HACEL device consisted of four successive layers, a top electrode, a fluorescent polymer/QD nanocomposite film including SWNTs as the light-emitting active layer, and an insulator formed on the transparent bottom electrode, as shown in **Figure 1**a. To control EL, single layer polymer/QDs hybrid blends of various pair combination were employed, including a blue emitting fluorescent polymer, PFO, and a green emitting poly[(9,9-di-n-octylfluorenyl-2,7-diyl)-alt-(benzo[2,1,3]thiadiazol-4,8-diyl)] (F8BT) and CdSe-ZnS core-shell type QDs with different color emission. Three kinds of CdSe/ZnS core-shell QDs with diameters of approximately 4, 6, and 8 nm were successfully synthesized by a previously reported method and exhibited their distinct photoluminescence (Supporting Information, S1 and S2).[6] As shown in the Figure 1b TEM image, for instance, orange QDs with a diameter of approximately 6 nm were apparent.

SWNTs dispersed with a conjugated block copolymer, poly(styrene-*block*-paraphenylene) (PS-*b*-PPP) were employed in the fluorescent polymer solution to provide more efficient field induced EL of either PFO or F8BT as explicitly demonstrated in our previous work.[13] As a representative example, SWNTs individually dispersed by PS-*b*-PPP were well mixed with PFO, leading to homogeneous composite films as shown in Figure 1c. Approximately 200-nm-thick hybrid film was spin-coated from a mixture of QDs and fluorescent polymer solutions on a SiO_2 insulating layer. Figure 1d shows the typical macrophase-separated microstructure of the QD/(SWNT/PS-*b*-PPP/PFO) nanohybrid film in which SWNTs were apparent throughout the film while QD aggregates with a typical size of approximately 400 nm in diameter were segregated. The phase segregated structure is also observed of a blend film prepared from a more dilute solution in the TEM micrograph in Figure 1e. Fabrication of the HACEL device was completed by thermally depositing 2-mm-wide periodic Au top electrodes on the nanohybrid film.

S. H. Cho, J. Sung, I. Hwang, R. H. Kim, Y. S. Choi, S. S. Jo, Prof. C. Park
Department of Materials Science and Engineering
Yonsei University, Seoul
120-749, Republic of Korea
E-mail: cmpark@yonsei.ac.kr
Prof. T.-W. Lee
Department of Materials Science and Engineering
Pohang University of Science and Technology (POSTECH)
San 31 Hyoja-dong, Nam-gu, Pohang
Gyungbuk 790-784, Republic of Korea.

DOI: 10.1002/adma.201201524

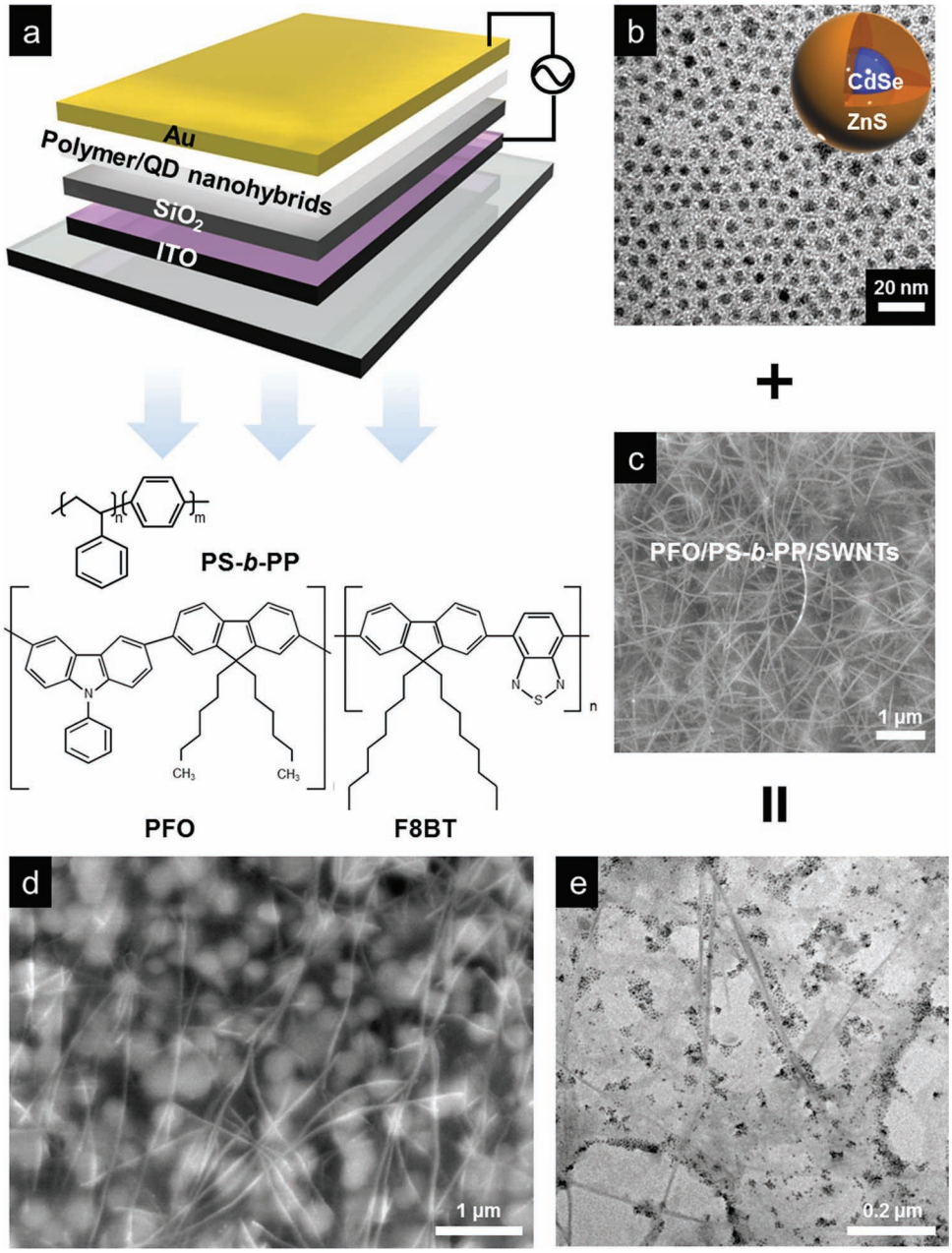

Figure 1. (a) Device architecture schematic of the HACEL device comprised of four layers: a hybrid nanocomposite of (SWNT/PS-*b*-PPP/fluorescent polymer)/(CdSe-ZnS QDs) blend, an insulating SiO_2 layer, and a transparent ITO bottom electrode stacked on top of the Au electrode. The molecular structures of F8BT and PFO as a light-emitting polymer and PS-*b*-PPP as dispersant for SWNT are shown. (b) Bright field TEM image of CdSe-ZnS QDs deposited on a Si wafer. The inset shows a schematic of core-shell type CdSe-ZnS QDs. (c) A representative SEM image showing the morphology of the SWNT/PS-*b*-PPP/PFO nanocomposite thin film spin-coated from THF solution containing 0.2 mg/mL SWNTs, 1 mg/mL PS-*b*-PPP, and 10 mg/mL PFO. Phase separated microstructures of (SWNT/PS-*b*-PPP/PFO)/(CdSe-ZnS QDs) blend films are shown in (d) SEM and (e) bright field TEM micrographs.

To ensure that the QDs were suitable for the emitting layer of the AC driven EL device and to examine how efficiently these devices emit light in an AC field, QD-only field-induced EL devices were investigated. Approximately 100-nm-thick QD films were spin coated on 200-nm-thick SiO_2 dielectric surfaces. All three QD-only AC devices in an AC field emitted the corresponding green, orange, or red light as shown in the photographs in **Figure 2**a. EL spectra obtained simultaneously with maximum emission wavelengths of 540, 590, and 640 nm shown in Figure 2b clearly suggest that colloidal QDs were well suited for AC driven full color EL operation. The field-induced operation of a QD only device was confirmed by the luminance-frequency behavior of the green QD device in which the luminescence increased with frequency to a maximum at

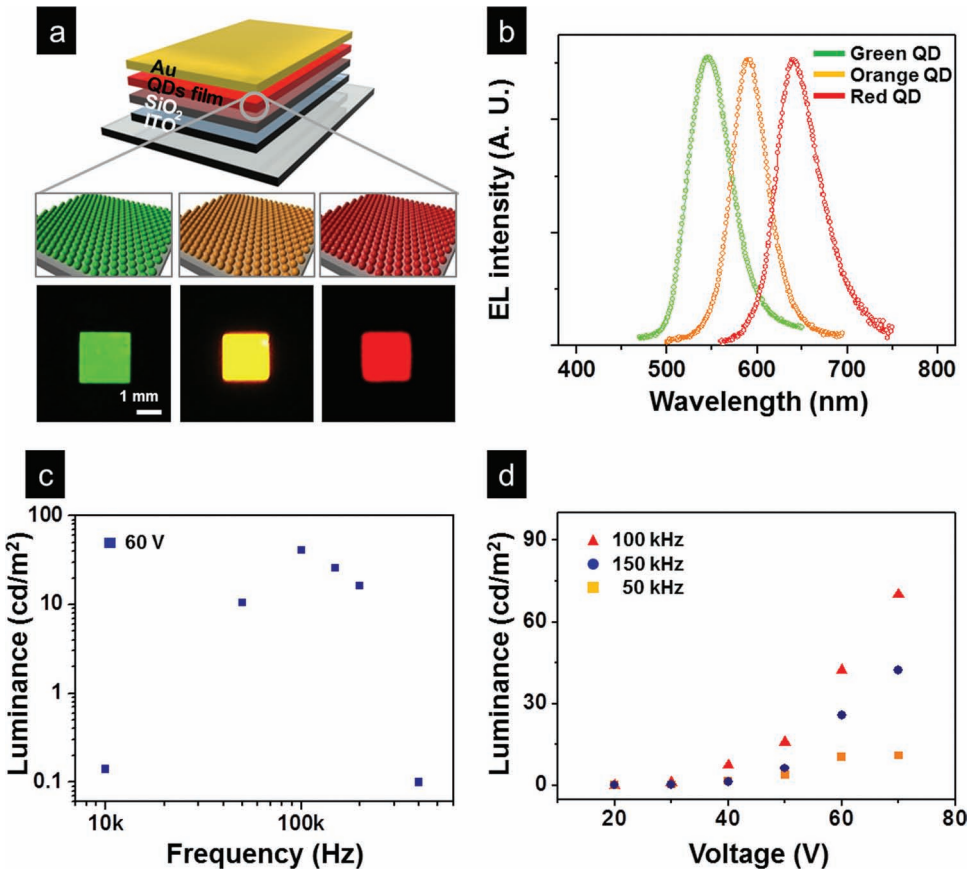

Figure 2. (a) Photographs of light emission from QD-only AC devices with different diameter CdSe-ZnS QDs. Green, orange, and red emissions arising from electroluminescence of CdSe-ZnS QDs of approximately 4, 6, and 8 nm in diameter, respectively, are apparent from 2 mm x 2 mm active cells of the AC devices schematically illustrated above the photographs. (b) EL spectra of QD-only AC devices with green, orange, and red CdSe-ZnS QDs. (c) Brightness and frequency plot of the QD-only AC device at a driving AC voltage of ±60 V. (d) Brightness and voltage relationships of the QD-only AC device at 50, 100, and 150 kHz.

approximately 100 kHz as shown in Figure 2c. In addition, the luminance-voltage behavior of the QD-only device with almost linear increase in intensity was very similar to a fluorescent polymer device,[13] as shown in Figure 2d. The maximum brightness of the device was approximately 70 cd/m^2 at an applied bias of ± 70 V and 100 kHz. It should be also noted that an attempt to enhance emission by mixing SWNTs with QD was not very effective mainly due to poor dispersion of SWNTs in QDs.

An inorganic/organic hybrid composite of QDs and fluorescent polymers offers an efficient route to fine color control as well as high brightness of emitted light at a low operating voltage.[22,23] To demonstrate our concept, we employed a single layered nanohybrid of F8BT and green QDs with SWNTs to facilitate the injection of carriers to the polymer. The HACEL device generated very bright greenish emission with operating voltage as shown in **Figure 3**a. The HACEL device initiated light emission at approximately 10 V, and its luminance increased almost linearly with applied voltage at 300 kHz reaching a maximum of approximately 620 cd/m^2 at ± 55 V as shown in Figure 3a. The HACEL device performance is indeed notable due to the cooperative emission from the two similar colors, resulting in its brightness much higher than the additive brightness of the two individual F8BT and QDs emissions as compared in intensity with EL spectra of individual emissions of QDs and F8BT previously obtained in Figure 3b.

The unique microstructure, with macro-phase separated QD aggregates embedded in the F8BT matrix along with the SWNT network as representatively shown in Figures 1d and e, is responsible for the independently mixed emission of green and super yellow light in the composite, respectively. Although fluorescence resonant energy transfer (FRET) occurs from the green colored QD domain to the F8BT matrix, it is limited to regions within the FRET distance, a few nanometers from the aggregated QD domains, making the contribution of FRET minimal. It is also notable that approximately 400 nm size aggregates of QDs well dispersed in the fluorescent polymer matrix have QDs individually packed with organic ligand, oleic acid, which can minimize EL quenching. The independent emission of our nanohybrid was confirmed with another blend of F8BT and red emitting QDs in which the two color emissions occurred with marginal FRET, again leading to highly enhanced cooperative EL (Supporting Information, S3).

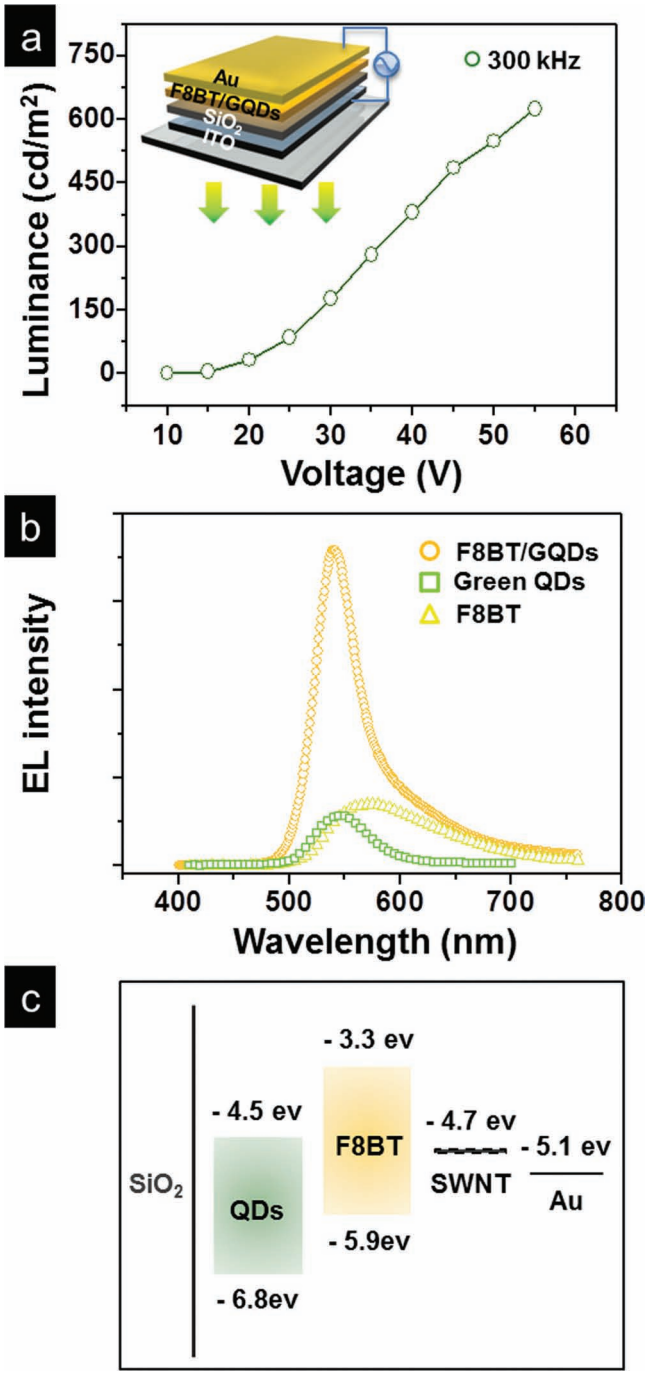

Figure 3. (a) A plot of brightness of a HACEL device consisting of Au/(SWNT/PS-*b*-PPP/F8BT)/(green CdSe-ZnS QDs) blend/200-nm-thick SiO_2/ITO as a function of applied voltage. (b) EL spectra of green QD-only AC device, F8BT-only AC device and HACEL device. Cooperative emission of two fluorescent materials from HACEL device is apparent in comparison with individual ELs of F8BT and green QDs. (c) Molecular orbital energy diagram of the components comprising a HACEL device.

A maximum brightness of approximately 620 cd/m^2 was obtained with the HACEL device while F8BT/PS-*b*-PPP/SWNT-only and QD-only devices fabricated with the same architecture as the HACEL device had maximum values of approximately 120 cd/m^2 at ±40 V and 70 cd/m^2 at ±70 V, respectively. The brightness of the HACEL was more than 3 times higher than the additive brightness of the two individual emissions. The enhanced emission may be attributed to smooth composite film in which F8BT played the role of polymer binder, rendering the composite film uniform in thickness during spin coating and thus improving the QD emission. In addition, the electrical band structure of the hybrid composite may be ascribed to the enhanced performance. In our composite, holes are primarily injected through the carbon nanotube network due to the lower injection barrier of SWNTs (work function: ~4.7 eV) than that of the QDs (HOMO: ~6.8 eV) with respect to the top Au electrode (work function: ~5.1 eV) as shown in Figure 3c. Subsequent transfer of the holes occurs to F8BT domains (HOMO: ~5.9 eV) in direct contact with the nanotubes. Considering that the HOMO of the green QDs is lower than that of F8BT, some of the holes transferred from the nanotubes not associated with electrons may subsequently migrate to the QDs with decent energy barrier. On the other hand, the electrons delivered from Au electrode to F8BT can be more easily transferred to QDs due to the LUMO of QDs (4.5 eV) lower than that of PFO (3.3 eV). An energy diagram of the F8BT/red QD device also supports our explanation (Supporting Information, S3). It is also plausible that the n-type semiconductor CdSe/ZnS QDs with relatively low conduction band as shown in Figure 3c could make electrons more efficiently injected from either SWNTs or Au top electrode to fluorescence polymer, F8BT, under AC field. The resulting plentiful excitons in F8BT regions lead to the EL intensity of F8BT in the composite brighter than that of a F8BT only AC EL device.

Our efficient control of AC EL with polymer/QD nanohybrids also provides a facile and robust way to fabricate white EL devices which have been in tremendous demand for next generation lighting and displays.[22–28] A novel HACEL device with a composite film of orange QDs and blue fluorescent polymer PFO generated a white emission in an AC field and displayed luminance-frequency behavior similar to other AC EL device with a maximum frequency of approximately 300 kHz, as shown in **Figure 4**a. As expected, the brightness of the hybrid device was significantly enhanced with a maximum of approximately 460 cd/m^2 at ± 30 V due to the cooperative emission of the two colors as shown in Figure 4b. (also see Supporting information, S4)

The EL spectrum in Figure 4c of the HACEL device containing a QD/PFO/SWNT composite clearly shows a broad emission of light with small intensity dips at approximately 430 nm and 590 nm. Compared with the individual EL spectra of orange emission from the QDs and blue emission from the PFO, shown below the hybrid spectrum in Figure 4c, our results with the hybrid device clearly indicate effective color mixing of the two spectra. The solid-state emission of our PFO in the AC EL device successfully provided the green emission additionally required for white emission of our HACEL device. It should be, however, noted that this green emission arose from increased defect emission in the solid film known as Keto defects[29] and was, in consequence, undesirable for high quality white EL. The Commission Internationale de l'Enclairage (CIE) coordinate of the device obtained simultaneously with the EL spectrum was (0.326, 0.338), which corresponds to typical white emission

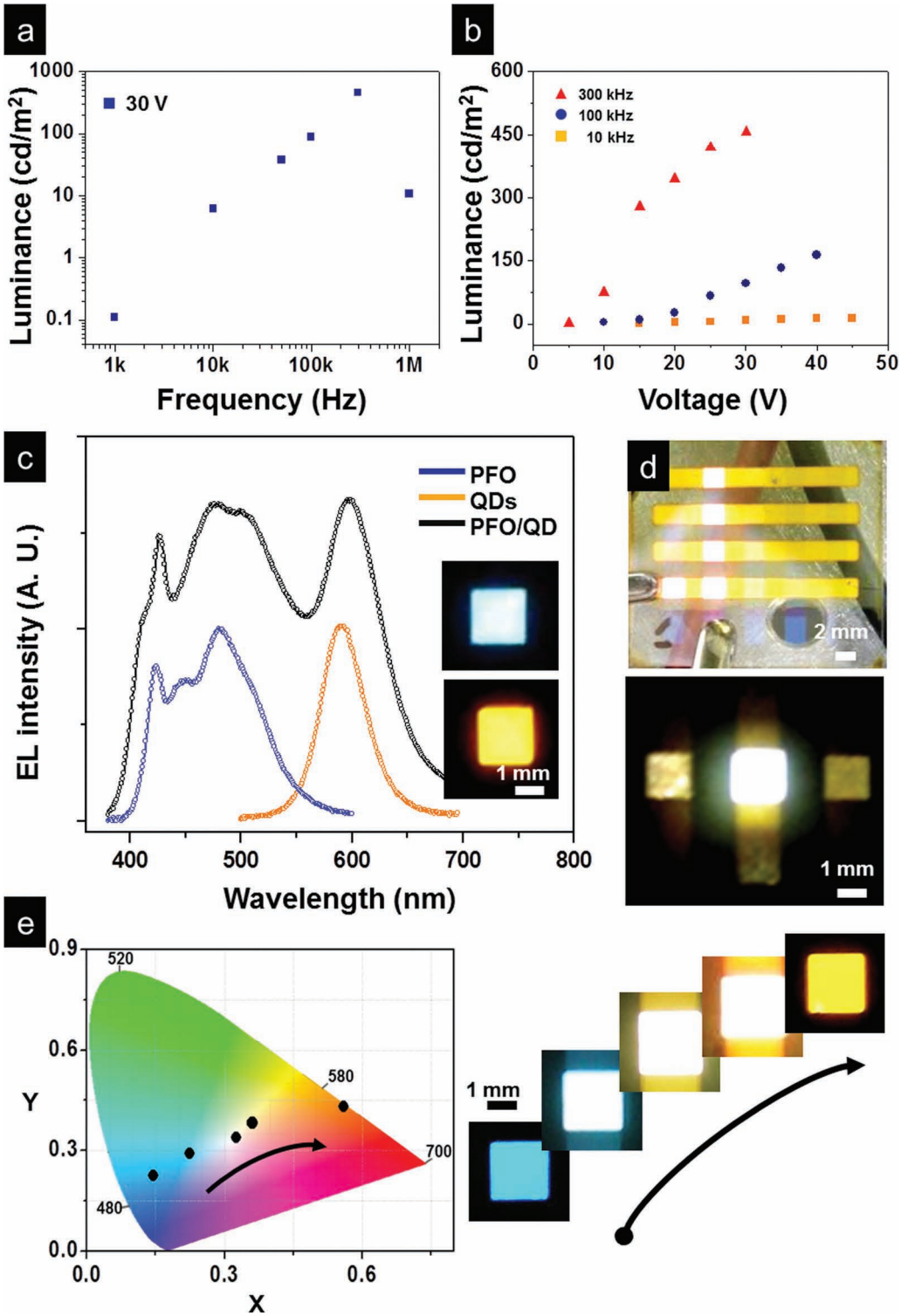

Figure 4. (a) Brightness and frequency plot of the white HACEL device consisting of Au/(SWNT/PS-*b*-PPP/PFO)/(CdSe-ZnS QDs) blend/200-nm-thick SiO_2/ITO at a driving AC voltage of ±30 V and (b) Brightness and voltage relationships of the white HACEL device at 10, 100, and 300 kHz. (c) EL spectrum (black color) of a white HACEL device. EL spectra of AC EL devices with emitting layers of PFO (blue color) and orange emitting CdSe-ZnS QDs (orange color) are also shown for comparison. EL spectra are arbitrarily shifted for clarity. Top and bottom photographs on the right-hand side exhibit light emission of AC EL devices containing PFO and CdSe-ZnS QDs, respectively. (d) Photographs of white light emission from the HACEL device. (e) The color space chromaticity diagram showing CIE coordinates of the emitting light from HACEL devices containing blend layers with different PFO to CdSe-ZnS QD ratios. A series of photographs of emission cells with different blend composites also exhibit facile color tuning as indicated by a black arrow.

although slight variation of CIE coordinates was observed as a function of AC voltage. (See Supporting information, S5) White emission of the HACEL device was readily visible even with the naked eye in common room light, as shown in Figure 4d. The highlighted cell in the bottom of Figure 4d clearly exhibited very bright white light emission under dark room conditions.

Strongly phase-separated composites with different blend ratios of QDs and PFO allowed easy generation of color tunable AC driven EL devices, as shown in Figure 4e. In addition to PFO and QD-only devices with blue and orange emissions and CIE coordinates of (0.145, 0.224) and (0.560, 0.431), respectively, we fabricated three additional AC driven devices with different PFO/QD blend ratios by controlling the amount of QDs to 50, 100, and 200 wt% with respect to PFO. The CIE coordinates of AC based devices containing the three different blend composites with ratios of PFO to QDs of 2, 1, and 0.5 were (0.224, 0.290), (0.326, 0.338), and (0.361, 0.382), respectively. The color space chromaticity diagram in Figure 4e clearly suggests that solution blending was an effective method for controlling emission color as a function of QDs in the composite as indicated by the black arrow in Figure 4e. A series of emission cell photographs with different blend composites in Figure 4e confirms the facile color tuning by blending (also see Supporting Information, S5).

In conclusion, we have effectively controlled AC driven electroluminescence from solution-processed colloidal quantum dots/fluorescent polymer hybrid emissive layers. Highly efficient cooperative emission of both quantum dots and fluorescent polymer in a flat, uniform hybrid film resulted in very bright AC EL of approximately 620 cd/m^2 which was more than 3 times brighter than the additive emission of the two individual emissions. Our strategy of hybrid AC driven EL for color mixing was successfully applied to realize novel white HACEL device. Furthermore, control of the blend ratio of QDs to fluorescent polymer provided a facile route to color tuning of the AC EL devices. Our field-induced AC driven EL devices, conveniently fabricated with conventional solution blending techniques, offer great potential for cost-effective next generation lighting and display products.

Experimental Section

Materials: The light-emitting fluorescent polymers, poly[(9,9-di-n-octylfluorenyl-2,7-diyl)-alt-(benzo[2,1,3]thiadiazol-4,8-diyl)] (F8BT) (M_n ~5000-8000) and poly(9,9-di-n-octylfluorenyl-2,7-diyl) (PFO) (MW: ~ 58200, PDI: ~3.7) were purchased from Sigma Aldrich. Colloidal CdSe/ZnS core-shell type quantum dots were synthesized with different diameters as previously described.[6] Briefly, for orange emitting QDs, 0.2 mmol of CdO, 4 mmol of ZnAc (zinc acetate) and 5 ml of oleic acid were mixed, and the solution was subsequently heated to 150 °C and degassed for 30 min, followed by heating to 300 °C while purging with N_2 gas. When the reaction reached 300 °C, 2 mL of trioctylphosphine (TOP) solution containing 31.2 mg of Se powder and 92.8 mg of S powder was quickly injected into the reaction flask for the synthesis of core-shell type CdSe/ZnS QDs. Purified arc-discharge single-walled carbon nanotubes (SWNTs) produced at Hanwha Nanotech, Grade ASP-100F, were used as received. Poly(styrene-*b*-paraphenylene) with polyphenylene rich in 1,4-addition (PS-*b*-PPP) was synthesized via dehydrogenation of poly(styrene-*b*-1,4-cyclohexadiene) by Polymer Source Inc., Doval, Canada. The molecular weights of PS and PPP were 4,800 g mol^{-1} and 1,100 g mol^{-1}, respectively. The polydispersity index (PDI) of PS-*b*-PPP was 1.10. All other materials were purchased from Aldrich and were used as received.

Preparations of Composites: Various amounts of SWNTs were dispersed in 1 mg/mL of PS-*b*-PPP THF solution. The appropriate amount of 0.5 mg/mL THF stock solutions of SWNTs prepared via brief sonication (NXP-1002, 60 Hz, 120 W, Kodo Technical Research Co., Ltd.) were added to PS-*b*-PPP solutions in THF, which allowed the concentration of the dispersed SWNTs in the polymer solution to be controlled. The mixtures were horn-sonicated for 5 min (VC 750, Sonics & Materials, Inc.), followed by bath sonication for 10 min. A fluorescent polymer was dissolved directly into the mixture, resulting in a fluorescent polymer/PS-*b*-PPP/SWNT composite solution. The solution was spin-coated on a SiO_2 insulator, leading to a composite film with 2 wt% SWNTs with respect to fluorescent polymer. Solutions of QDs of different diameters in THF were also spin-coated on SiO_2 insulator surfaces for QD-only AC devices. For the hybrid EL device, 1 wt% QD dispersed in hexane was centrifuged at 15000 rpm for 60 min to remove residual hexane, and then the QDs were mixed with fluorescent polymer/PS-*b*-PPP/SWNT composite solutions, followed by bath sonication for 10 min. The mixtures of fluorescent polymer/PS-*b*-PPP/SWNT and QDs with various blend compositions prepared in THF were spin-coated on insulating layers.

Light-Emitting Device Fabrication: Light-emitting devices were based on a layered structure of ITO/insulator/emissive layer/metal. A 200-nm-thick SiO_2 insulating layer was deposited onto glass substrates with pre-patterned 2-mm-wide strips of transparent bottom electrodes made of indium tin oxide (ITO). Bi-layered SiO_2/ITO glass substrates were purchased from Freemteck Inc., South Korea. A 200-nm-thick SiO_2 layer was deposited onto the ITO surface with low-pressure plasma (10^{-5} Torr) at 400 °C using plasma-enhanced chemical vapor deposition. The sheet resistance of the ITO substrate was approximately 10 Ω/□. The emissive composite films were prepared by spin-coating the composite solutions onto the insulating layers at 1000 rpm. Light-emitting devices were completed by depositing 2-mm-wide strips of Au top electrodes via thermal evaporation (Thermal Evaporator: MEP 5000, SNTEK Co., Ltd.) through a shadow Sus-Mask under a pressure of 10^{-6} mbar at a rate of 0.1 nm/sec, resulting in light-emitting 2 mm × 2 mm square cells at the intersection of the bottom and top electrode strips. An Agilent 20 MHz function generator with a voltage amplifier was used to power the light-emitting devices.

Characterization Methods: The nanostructures of fluorescent polymer/PS-*b*-PPP/SWNTs, QDs, and their hybrid blend nanocomposite films were analyzed using a tapping mode atomic force microscope (AFM) (Nanoscope IV^a Digital Instruments) in height and phase contrast, a field-emission scanning electron microscope (FESEM) (JEOL JSM-600F), and a high-resolution transmission electron microscope (HRTEM) (JEOL 2100F) in bright field mode. Optical absorbance and fluorescence spectra for solutions and films were obtained using a JASCO V-530 UV visible spectrophotometer and a Varian Cary Eclipse fluorescence spectrophotometer, respectively. Both brightness and electroluminescence spectra of devices were obtained with a spectroradiometer (Konica CS 2000). All measurements were performed in a dark box at room temperature in air.

Supporting Information

Supporting Information is available from the Wiley Online Library or from the author.

Acknowledgements

This project was supported by DAPA and ADD, and the Converging Research Center Program through the Ministry of Education, Science and Technology (No.2011K000631). This work was supported by the project

of Global Ph.D. Fellowship which National Research Foundation of Korea conducts from 2011. This research was also supported by the Second Stage of the Brain Korea 21 Project in 2006 and a Korea Science and Engineering Foundation (KOSEF) grant, funded by the Ministry of Science and Technology (MEST), Republic of Korea (No. R11-2007-050-03001-0).

Received: April 17, 2012
Revised: June 4, 2012
Published online: July 12, 2012

[1] T.-H. Kim, K.-S. Cho, E. K. Lee, S. J. Lee, J. Chae, J. W. Kim, D. H. Kim, J.-Y. Kwon, G. Amaratunga, S. Y. Lee, B. L. Choi, Y. Kuk, J. M. Kim, K. Kim, *Nat. Photon.* **2011**, *5*, 176.
[2] Q. Sun, Y. A. Wang, L. S. Li, D. Wang, T. Zhu, J. Xu, C. Yang, Y. Li, *Nat. Photon.* **2007**, *1*, 717.
[3] S. Coe, W.-K. Woo, M. Bawendi, V. Bulovi , *Nature* **2002**, *420*, 800.
[4] K.-S. Cho, E. K. Lee, W. J. Joo, E. Jang, T. H. Kim, S. J. Lee, S. J. Kwon, J. Y. Han, B. K. Kim, B. L. Choi, J. M. Kim, *Nat. Photon.* **2009**, *3*, 341.
[5] R. H. Friend, R. W. Gymer, A. B. Holmes, J. H. Burroughes, R. N. Marks, C. Taliani, D. D. C. Bradley, D. A. Dos Santos, J. L. Bredas, M. Logdlund, W. R. Salaneck, *Nature* **1999**, *397*, 121.
[6] W. K. Bae, K. Char, H. Hur, S. Lee, *Chem. Mater.* **2008**, *20*, 531.
[7] J.-M. Caruge, J. E. Halpert, V. Wood, M. G. Bawendi, V. Bulovi , *Nat. Photon.* **2008**, *2*, 247.
[8] C. W. Tang, S. A. VanSlyke, *Appl. Phys. Lett.* **1987**, *51*, 913.
[9] L. Qian, Y. Zheng, J. Xue, P. H. Holloway, *Nat. Photon.* **2011**, *5*, 543.
[10] W. K. Bae, J. Kwak, J. Lim, D. Lee, M. K. Nam, K. Char, C. Lee, S. Lee, *Nano Lett.* **2010**, *10*, 2368.
[11] T. W. Lee, J. Zaumseil, S. H. Kim, J. W. P. Hsu, *Adv. Mater.* **2004**, *16*, 2040.
[12] V. Wood, M. J. Panzer, J. Chen, M. S. Bradley, J. E. Halpert, M. G. Bawendi, V. Bulovi , *Adv. Mater.* **2009**, *21*, 2151.
[13] J. Sung, Y. S. Choi, S. J. Kang, S. H. Cho, T.-W. Lee, C. Park, *Nano Lett.* **2011**, *11*, 966–972.
[14] V. Wood, M. J. Panzer, D. Bozyigit, Y. Shirasaki, I. Rousseau, S. Geyer, M. G. Bawendi, V. Bulovi , *Nano Lett.* **2011**, *11*, 2927.
[15] A. Perumal, M. Frobel, S. gorantla, T. Gemming, Bjorn Lussem, Jurgen Eckert, K. Leo, *Adv. Funct. Mater.* **2012**, *22*, 210.
[16] G. J. Destriau, *Chim. Phys.* **1936**, *33*, 587.
[17] D. C. Krupka, *J. Appl. Phys.* **1972**, *43*, 476.
[18] X. L. Xu, X. H. Chen, Y. B. Hou, Z. Xu, X. H. Yang, S. G. Yin, Z. J. Wang, X. R. Xu, S. P. Lau, B. K. Tay, *Chem. Phys. Lett.* **2000**, *325*, 420.
[19] S. Y. Yang, L. Qian, F. Teng, Z. Xu, X. R. Xu, *J. Appl. Phys.* **2005**, *97*, 126101.
[20] G. Gu, G. Parthasarathy, P. E. Burrows, P. Tian, I. G. Hill, A. Kahn, S. R. Forrest, *J. Appl. Phys.* **1999**, *86*, 4067.
[21] T. Tsutsui, S. Lee, K. Fujita, *Appl. Phys. Lett.* **2004**, *85*, 2382.
[22] Y. Li, A. Rizzo, R. Cingolani, G. Gigli, *Adv. Mater.* **2006**, *18*, 2545.
[23] J. H. Park, J. Y. Kim, B. D. Chin, Y. C. Kim, J. K. Kim, O. O. Park, *Nanotechnology* **2004**, *15*, 1217.
[24] L. Chen, P. Li, Y. Cheng, Z. Xie, L. Wang, X. Jing, F. Wang, *Adv. Mater.* **2011**, *23*, 2986.
[25] Y. Li, A. Rizzo, M. Mazzeo, L. Carbone, L. Manna, R. Cingolani, G. Giglia, *J. Appl. Phys.* **2005**, *97*, 113501.
[26] H. S. Jang, H. Yang, S. W. Kim, J. Y. Han, S.-G. Lee, D. Y. Jeon, *Adv. Mater.* **2008**, *20*, 2696.
[27] P. O. Anikeeva, J. E. Halpert, M. G. Bawendi, V. Bulovi , *Nano Lett.* **2007**, *7*, 2196–2200.
[28] G. M. Farinola, R. Ragni, *Chem. Soc. Rev.* **2011**, *40*, 3467.
[29] E. J. W. List, R. Guentner, P. S. D. Freitas, U. Scherf, *Adv. Mater.* **2002**, *14*, 374.